Raman active modes in single-walled boron nitride nanotube bundles

B. Fakrach, A. Rahmani, H. Chadli, K. Sbai and M.Bentaleb

Laboratoire de Physique des mat´eriaux et Mod´elisation des Systèmes,
UniversitéMoulay Ismaïl,
Faculté des Sciences (Unité Associée au CNRST-URAC08), BP 11201,
Zitoune, 50000 Meknès, Morocco

(Dated: October 10, 2011)

Abstract: We use the spectral moments method in the framework of the bond-polarization theory to calculate polarized nonresonant Raman spectra of chiral and achiral bundles of single walled boron nitride nanotubes (BWBNNTs) as a function of their diameter and chirality. The Spectra are computed for infinite size of BWBNNTs. We used a Lennard-Jones potential to describe the van der waals intertube interactions between tubes in a bundle. We show that the Raman active modes in the low wave number region are very sensitive to the nanotube diameter. We found that for infinite nanotube bundles, additional Radial Breathing Like mode appears in the low wave number region. These results are useful to interpret the experimental Raman spectra of BWBNNTs.

PACS numbers: 61.46.Fg, 63.22+m, 61.43.Bn

I. INTRODUCTION

The discovery of carbon nanotubes by Iijima [1] was followed by perspectives of similar nanostructures to be formed by non-carbon-layered structures. Boron nitride nanotubes (BNNTs) were first predicted to be stable structure based on tight-binding [2] and first-principal calculations due to their unique physical and chemical properties, [3] the BNNTs open new possibilities for technological applications in the nanoscale dimension which are not possible with carbon nanotubes. Chemical inertness and a strong resistance to oxidation for example, make BNNTs highly appropriate for the construction of insulating nanocables, a subject that has been attracting increased attention [4, 5]. The experiments have shown that BNNTs contain unique properties and could be applied in various branch of material science [6]. In contrast to Carbon nanotubes which can be either metal or semi-conductor, BNNTs are always semiconducting with a large band gap of about 5.5 eV [2, 3]. In 1995, the first synthesis of BNNTs was realized with arc-charging method using the boron nitride (BN) electrode packed into a metal casing [7-9]. Other preparation methods have been developed subsequently, such as arc-melting [10], high temperature chemical reaction [5, 11-14], carbon nanotube templates [15], ball-milling [16], and laser ablating [17, 18].

Raman spectroscopy is known the most efficient tools for investigating the vibrational properties of materials in relation to their structural and electronic properties. Experimentally, the Raman spectrum of the synthesized BNNT is dominated by a strong characteristic peak located around 1366 cm^{-1}. Lee et al [14] have presented a growth approach of boron nitride nanotubes. The typical BNNT diameters and lengths are ranged from 10 to 100 nm and greater than 10 µm, respectively. The Raman scattering spectrum of purified BNNTs exhibits only one Raman active mode, E_{2g}, in the range of 1100-1600 cm^{-1}. The E_{2g} mode of boron nitride is due to the in-plane atomic displacement of B and N atoms against each other. This peak is located at 1356 cm^{-1} by Lim et al [16], at 1367 cm^{-1} by Lee et al [14], at 1366 cm^{-1} by Naumov et al [19], at 1365 cm^{-1} by Sunil et al [20], at 1368.8 cm^{-1} by Singhal et al [21] . Recently, Guo et al [22] reported interesting results synthesis of BNNTs, they either appear in bundles with a width close to 50-70 nm or as a single tube with a diameter around 5-20 nm. In this context, their characterization through vibrational spectroscopies is expected to play an important role. The Raman active modes of individual single BNNTs have been predicted by different theoretical approaches: zone-folding combined with bond polarizability parameters of carbon [3, 7, 23], tight binding approach [24], ab initio calculations [25, 26], and our model [27].

The moments method was initially developed by different authors studying electronic properties in solid-state physics [28, 29]. A few years ago, the spectral moment's method (SMM) was shown to be a powerful tool for determining infrared absorption, Raman scattering, and inelastic neutron scattering spectra of harmonic systems [30-34]. This method can be applied to large systems, whatever the type of atomic forces, the spatial dimension, and structure of the material. This method was previously used to study the dynamical properties of different disordered systems having more than 10^6 degrees of freedom, as it is the case with Sierpinski

gaskets [31], silica aerogels [32] and diffusion-limited cluster-cluster aggregates [33, 34]. The SMM was recently used to calculate IR and Raman spectra of carbon nanotubes [35-38], peapods [39-41] and SWBNNT's [27, 42].

In this paper, in order to complete our study about the vibrations of SWBNNT's, we investigate the bundling effect on the Raman spectra of SWBNNT's. We present calculations of the nonresonant Raman spectrum of SWBNNT's bundles using the spectral moments method. Our calculations do not predict the changes of the spectra with the excitation energy or the relative intensity of the different modes for a fixed excitation energy. Nevertheless, These calculations were performed for a large collection of SWBNNT's bundles with various structural properties (diameter and chirality). These predictions are useful to interpret the experimental Raman spectra of SWBNNT's bundles.

II. MODELS AND METHOD

A SWBNNT structure can be obtained by rolling a single hexagonal BN sheet. Following the usual terminology of reference [43], the tube can be specified by integers (n,m) which define the translation vector between the two points. Alternatively, the tube can be described by its diameter D and the chiral angle θ, which is the angle between the tube circumference and the nearest zigzag of B-N bonds. According to the chirality, SWBNNT's can be classified into two types: achiral tubes, including armchair (n,n) plus zigzag (n,0), and chiral tubes (n,m= n = 0). The diameter D and the chiral angle θ of a SWBNNT are given by:

$$D = \frac{a}{\pi}\sqrt{n^2 + m^2 + m.n} \qquad (1)$$

With a=1.435Å

$$\theta = \tan^{-1}\left[\frac{\sqrt{3}m}{(m+2n)}\right] \qquad (2)$$

When SWBNNTs are closely packed together, a three-dimensional boron nitride bundle is formed. From the diffrac-tion profile of the crystalline ropes of SWBNNTs, it has been previously reported that these systems can be represented by two-dimensional infinite trigonal lattices of uniform cylinders. For a finite-size bundle, the nanotubes were placed parallel to one another on a finite-size trigonal array of cell parameter $a_0 = D + d_{t-t}$, where d_{t-t} =3.35Å represents the intertube spacing [13, 44]. The number of tubes par bundle is called N_t.

In the present work, we calculate the polarized Raman spectra for finite and infinite bundles. The intratube interactions are described by using the same force constant set as used in our calculations of the Infrared spectra of SWBNNTs [42].

A Lennard-Jones potential:

$$U_{LJ} = 4\varepsilon\left[\left(\frac{\sigma}{R}\right)^{12} - \left(\frac{\sigma}{R}\right)^{6}\right] \qquad (3)$$

is used to describe the van der waals intertube interactions between the tubes in a bundle. In this work, the parameters for LJ12-6 potential are ε_{Boron}=0.004116eV, σ_{Boron}=3.453Å and $\varepsilon_{Nitrogen}$=0.004116eV, $\sigma_{Nitrogen}$=3.365Å [44, 45]. The Boron-Nitrogen and Nitrogen-Boron parameters were derived using the Lorentz-Berthelot mixing rules, $\varepsilon_{AB} = \left(\varepsilon_A + \varepsilon_B\right)^{\frac{1}{2}}$ and $\sigma_{AB} = (\sigma_A + \sigma_B)/2$. A usual method to calculate the Raman spectrum requires, the eigenvalues and the eigenvectors which can be obtained by direct diagonalizatin of the dynamical matrix of the system. However when the system contains a large number of atoms, as for long finite SWBNNT bundles, the dynamical matrix is very large and its diagonalization fails or requires long computing time. By contrast, the spectral moments method allows to compute directly the Raman spectrum of very large harmonic systems without any diagonalization of the dynamical matrix [30, 32]. Otherwise, for small samples, both approaches lead exactly to the same position and intensity for the different peaks. The spectram moment's method consist of developing the resolvent R(z) of the response of the system, J(u) which can be written as ($z = u + i\varepsilon$) [30, 32]

$$J(u) = -\frac{1}{\pi}\lim_{\varepsilon\to 0^+}\mathrm{Im}\left[R(z)\right] \qquad (4)$$

in a continued fraction:

$$R(z) = \cfrac{b_0}{z - a_1 - \cfrac{b_1}{z - a_2 - \cfrac{b_2}{z - a_3 - .... \cfrac{b_n}{z - a_{n+1}}}}} \qquad (5)$$

Where the coefficients a_n and b_n are given by:

$$a_{n+1} = \frac{\bar{\upsilon}_n}{\upsilon_n}; b_n = \frac{\upsilon_n}{\upsilon_{n-1}} \qquad (6)$$

The spectral generalized moments ν_n and $\bar{\nu}_n$ of J(u) are directly obtained from the dynamical matrix $\tilde{D}$. As shown in our earlier works [32, 46], a sharp truncation of the continued fraction leads to the appearance of sharp lines in the calculated low-frequency spectrum. On the other hand, the calculations of Raman and infrared spectra show that a limited number of moments are sufficient to obtain the frequency of active modes with a good accuracy. In this work 500 moments have been used.

RESULTS AND DISCUSSION

Here we report calculations for polarized Raman spectra of achiral and chiral BWBNNTs of different diameters and lengths performed using the spectral moments method. The mode frequency is directly obtained from the position of the peak in the calculated Raman spectrum. The line shape of each peak is assumed to be Lorentzian and the linewidth is fixed at 1.7 cm^{-1}. For each BWBNNTs, the intensities of the different polarized spectra are normalized and can be compared. In all our calculations, we consider the Z nanotube axis is to be along z axis, and the X nanotube axis is to be along the x axis of the laboratory reference frame. The laser beam is kept along the y axis. Calculations are performed on infinite SWBNNT's which are obtained by applying periodic conditions on the unit cells of the nanotubes. To obtain a finite nanotube with open ends, we suppress simply the periodic conditions and translate the unit cell along the tube axis.

Three geometrical configurations are considered: in the ZZ configuration, both incident and scattered polarizations are along the Z axis and, for ZX (XY) configuration, the incident and scattered polarizations are along the Z(X) and X(Y) axes respectively. In this section, we report the calculated Raman spectra for infinite and finite isolated SWBNNTs bundles of different sizes. The dependence of the Raman spectrum as a function of tube diameter and chirality is investigated.

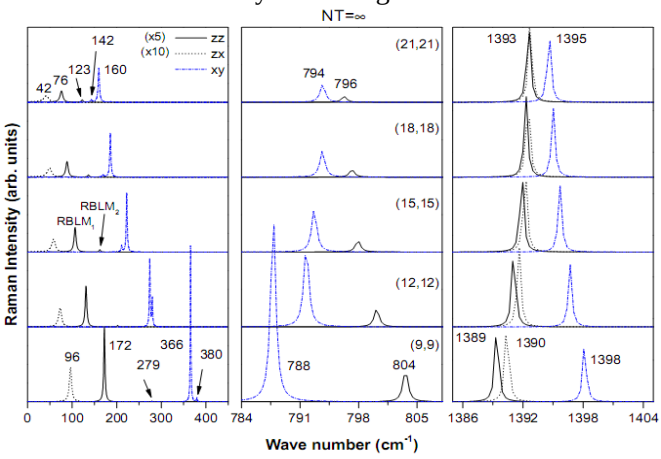

Figure 1. The ZZ, ZX and XY calculated Raman spectra of (n,n) SWBNNT crystal for n=9, 12, 15, 18 and 21 from bottom to top.

Firstly, the calculations are performed on infinitely homogeneous bundles (crystal: N T $= \infty$) of SWBNNTs of several diameters. We recall that infinite SWBNNTs are obtained by applying periodic conditions on unit cells of the studied nanotubes. The results for typical armchair tubes (9,9), (12,12), (15,15), (18,18) and (21,21) are reported in figure 1. The ZZ, ZX and XY Raman spectra are displayed in the low wave number or breating-like mode (BLM: on the left) region, intermediate (on the intermediate) region and high wave number or tangential-like mode (TLM: on the right) region. In the TLM region, all spectra display one peak corresponding to A_{1g} (ZZ), E_{1g} (ZX) and E_{2g} (XY) modes. Shift up for A_{1g} and E_{1g} modes are observed when the tube diameter increases, and shift down for E_{2g} modes. In the Intermediate region, spectra display one peak only for A_{1g} and E_{2g} modes and no E_{1g} mode appears for ZX polarized Raman spectra. We observe a downshift for A_{1g} and upshift for E_{2g} modes with increasing tube diameter respectively. In the BLM region spectra are dominated by one peak E_{1g} and two modes E_{2g} for ZX and XY polarization. The ZZ spectra exibit also two peaks denoted here as RBLM (for radial breating-like mode) and BBLM (for bundle breating-like mode). We observe that all modes downshift with increasing tube diameters. The comparison between the Raman spectra of SWBNNTs and BWBNNTs show the additional modes are observed in the BLM region with low intensity (most significant: for ZZ spectra a second mode BBLM at wave number higher than that of RBLM one. In the BLM and intermediate regions, the intensity of all Raman active modes decreases with increasing tube diameter. From this study, it is shown that the low wave number modes are likely the most influenced modes by the diameter variation in comparison to the intermediate and high wave number ones.

To illustrate the BLM wave number dependence on nanotube diameter, we have reported in figure 2, the evolution of the calculated wave numbers of the Raman active modes (*) symbols for RBM mode of isoalted SWBNNTs and (•) and (x) symbols for RBLM and BBLM modes of SWBNNT bundles respectively. We show that the wave number modes obey the A/D law, with A close to the value 198.68, 205.84, and 316.84 cm^{-1} nm for RBM, RBLM and BBLM respectively. This behavior is close to the one calculated for the Raman-active breathing modes using the same approach [27] for SWBNNT. In agreement with the reference [47] , the fitting constants of radial breathing modes in bundles are consistent with previous calculations with values 207.6, 220.2 nm cm^{-1} for the zigzag and armchair tubes, respectively. In comparison with carbon nanotubes, a similar A/D trend has been obtained [36, 47], with fitting constants greater than those of BWBNNTs. These results imply that our fitted constants could be used to predict low wave number for large diameter tubes.

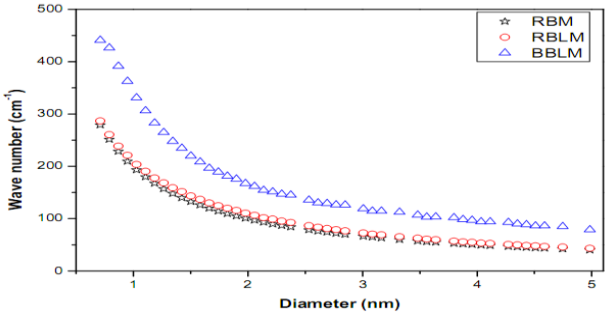

Figure 2. Diameter dependence of the wave number ZZ Raman active modes for isolated and bundles SWBNNTs.

In the following, we focus on the chirality dependence of the ZZ polarized Raman spectra of BWBNNTs in the BLM and TLM regions. Calculations were performed for four values of the chiral angle θ (0, 10, 20, and 30), associated with (16,0), (14,3), (12,6), and (9,9) nanotubes bundles, respectively (figure 3). In the TLM region, for zigzag (θ=0) and armchair (θ=30) tubes, spectra are featured by a strong peak assigned to A_{1g} tangential modes. Let us call ω_z and ω_a the wave number of the zigzag and armchair TLM mode, respectively. The increase of θ from 0 to 30 leads to the appearance of two peaks at wave numbers close to ω_z and ω_a. The intensity of these peaks shifts from the one located around ω_z to that located around ω_a when increasing θ. For the armchair tube, a single peak located at ω_a has nonzero intensity. In contrast to SWBNNT, We can note that the wave numbers of BLM modes are sensitive to the chirality. When the increase of θ from 0 to 30, the modes RBLM and BBLM up shift from 168 and 265 to 172 and 279 respectively.

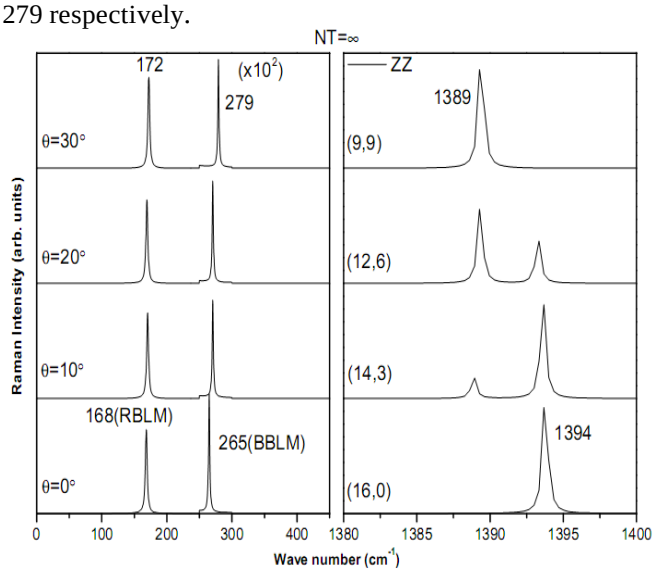

Figure 3. The chirality dependence of the BLM (left) and TLM (right) Raman spectra for symmetry ZZ, calculations were performed for four values of the chiral angle θ (0, 10, 20, and 30), associated with (16,0), (14,3), (12,6), and (9,9) nanotubes bundles, respectively.

III. CONCLUSION

In conclusion, we have investigated Raman spectra of homogeneous bundles of SWBNNTs. Thanks to the spectral moment's method, we have investigated bundles consisting of more than 100 SWBNNTs of several diameter and chirality. Bundling effects are observed essentially in the low wave number regions with additional Bundle breathing like modes, which can be considered in the analysis of experimental data.

IV. ACKNOWLEDGEMENTS

The work was supported by the Morocco-Spain Inter academic Mixed Committee and a CNRS-France/CNRST- Morocco agreement.

[1]. S. Iijima, Nature (London) 354,56 (1991).

[2]. Rubio. A, Corkill J L, Cohen M L 1994 Phys. Rev. B 49 5081.

[3]. X. Blase , A.G. Rubio, S. Louie, M.L. Cohen, Eruophys. Lett. 28 (1994) 335.

[4]. D. Golberg, F.-F. Xu, Y. Bando, Appl. Phys. A 76 (2003) 479.

[5]. C. Tang, Y. Bando, D. Golberg, X. Ding, S. Qi, J. Phys. Chem. 107 (2003) 6539. 601.

[6]. J. Wang, V.K. Kayastha, Y.K. Yap, Z. Fan, J.G. Lu, Z. Pan, I.N. Ivanov, A.A. Puretzky, D.B. Geohegan, Nano Lett. 5 (2005) 2528. 1699.

[7]. Chopra N G, Luyken R J, Cherrey K, Crespi V H, Louie S G and Zettl A 1995 Science 269 966.

[8]. Terrones M, Hsua W K, Terrones H, Zhang J P, Ramos S, Hare J P, Castillo R, Prassides K, Cheetham A K, Kroto H W and Walton D R M 1996 Chem. Phys. Lett. 259 568.

[9]. Loiseau A, Willaime F, Demoncy N, Hug G and Pascard H 1996 Phys. Rev. Lett. 76 4737.

[10]. (a) T. Hirano, T. Oku, K. Suganuma, Diamond Relat. Mater. 9 (2000) 625; (b) M. Kuno, T. Oku, K. Suganuma, Diamond Relat. Mater. 10 (2001) 1231.

[11]. Lourie O R, Jones C R, Bartlett B M, Gibbons P C, Ruoff R S and Buhro W E 2000 Chem. Mater. 12 1808.

[12]. Zhi C, Bando Y, Tan C, Golberg D 2005 Solid State Commun. 135 67.

[13]. Lin F H, Hsu C-K,Tang T-P,Kang P-L, Yang F-F 2008 Materials Chemistry and Physics 107 115-121.

[14]. Lee C H, Wang J, Kayatsha V K, Huang J Y and Yap Y K 2008 Nanotechnology 19 455605.

[15]. (a) W. Han, Y. Bando, K. Kurashima, T. Sato, Appl. Phys. Lett. 73 (1998) 3085; (b) D. Golberg, Y. Bando, W. Han, K. Kurashima, T. Sato, Chem. Phys. Lett. 308 (1999) 337; (c) D. Golberg, Y. Bando, K. Kurashima, T. Sato, Chem. Phys. Lett. 323 (2000) 185.

[16]. Lim S H, Luo J, Ji Wei, Lin J 2007 Catalysis Today. 120 346-350.

[17]. (a) D. Golberg, Y. Bando, M. Eremets, K. Takemura, K. Kurashima, H. Yusa, Appl. Phys. Lett. 69 (1996) 2045;(b) D.P. Yu, X.S. Sun, C.S. Lee, I. Bello, S.T. Lee, H.D. Gu, K.M. Leung, G.W. Zhou, Z.F. Dong, Z. Zhang, Appl. Phys. Lett. 72 (1998) 1966.

[18]. Yu D P, Sun X S, Lee C S, Bello I, Lee S T, Gu H D, Leung K M, Zhou G W, Dong Z F and Zhang Z 1998 Appl.Phys. Lett. 72 1966.

[19]. Naumov V G and al 2009 Laser Physics 19 1198-1200.

[20]. Sunil Kumar Singhal, Avanish Kumar Srivastava, Nita Dilawar, Anil Kumar Gupta, (2009)J Nanopart Res.

[21]. S. K. Singhal, A. K. Srivastava, Anil K. Gupta, Z. G. Chen, (2009)J Nanopart Res.

[22]. Guo L, Singh R N 2009 Phys E 41 448-453.

[23]. Popov V N 2003 Phys. Rev. B 67 085408.

[24]. Sanchez-Portal D and Hernandez E 2002 Phys.Rev. B 66 235415.

[25]. Wirtz L, Rubio A, de la Concha R A, and Loiseau A 2003 Phys. Rev. B 68 045425.

[26]. Wirtz L and Rubio A 2003 Ieee transactions on nanotechnology. 2 4.

[27]. Fakrach B, Rahmani A, Chadli H, Sbai K and Sauvajol J-L 2009 Phys E 41 1800-1805.

[28]. P.H. Lambin and J.P. Gaspard, Phys. Rev. B 26, 4356 (1982), and references therein.

[29]. E. Jurczek, Phys. Rev. B 32, 4208 (1985), and references therein.

[30]. C. Benoit, E. Royer, and G. Poussigue, J. Phys.: Condens. Matter 4, 3125 (1992).

135

[31]. C. Benoit, G. Poussigue, and A. As
Phys.: Condens. Matter 4, 3153 (1992).

[32]. A. Rahmani, C. Benoit and G. Poussigue, J. Phys.: Condens. Matter 5 7941 (1993).

[33]. A. Rahmani, C. Benoit, R. Jullien, G. Poussigue, and A. Sakout, J. Phys.: Condens. Matter 9, 2149 (1997).

[34]. A. Rahmani, P. Jund, C. Benoit, and R. Jullien, J. Phys.: Condens. Matter 13, 5413 (2001).

[35]. A. Rahmani, J.-L. Sauvajol,1 S. Rols,3 and C.Benoit, Phys. Rev. B 66, 125404 (2002).

[36]. K. Sbai, A. Rahmani, H. Chadli, J.-L. Bantignies, P. Hermet, and J.-L. Sauvajol, J. Phys. Chem. B 110, 12388-12393 (2006).

[37]. K. Sbai, A. Rahmani, H. Chadli and J.-L. Sauvajol, J. Phys.: Condens. Matter 20, 015204 (2008).

[38]. K. Sbai, A. Rahmani, H. Chadli and J.-L. Sauvajol, J. Phys.: Condens. Matter 21, 045302(2009).

[39]. J. Cambedouzou, J.-L. Sauvajol, A. Rahmani, E. Flahaut, A. Peigney, and C. Laurent, Phys. Rev. B 69, 235422 (2004).

[40]. H. Chadli, A. Rahmani, K. Sbai, P. Hermet, S. Rols, J-L. Sauvajol, Phys. Rev. B 74, 205412 (2006).

[41]. A. Rahmani and H. Chadli, Handbook of Nanophysics: Structure and vibrations in C60 carbon peapods, p 46.1-29 (Taylor and Francis Publisher, CRC Press, New York, 2010).

[42]. B. Fakrach et al. Phys. Rev. B, Infrared spectrum of finite and infinite single-walled boron nitride nanotube, (submitted).

[43]. R. Saito, G. Dresselhaus, and M.S. Dresselhaus, Physical properties of Carbon nanotubes (Imperial College, London, 1998).

[44]. Lee J H, 2006 Journal of the Korean Physical Society 49 172-176.

[45]. Kang J W and Hwang H J, 2004 J. Phys: Condens. Matter 16 3901-3908.

[46]. Rahmani A, Sauvajol J L, Rols S and Benoit C 2002 Phys. Rev. B 66 125404.

[47]. R. Akdim, R. Pachter, Duan Xiaofeng, W. W. Adams, Phys. Rev. B 67, 245404 (2003).

